but they provide no information on the identity or fate of species between $A,B(PO)_n$ or $C(OP)_n$ and final products.

Acknowledgment. This work was supported financially by Grant RR07143 from the Department of Health and Human Services and by Grant INT-8512210 from the National Science Foundation, which are gratefully acknowledged. We thank Professors Ahmed El-Toukhy, John Groves, and Kenneth Karlin for valuable discussions, Professor Conrad Jankowski for software development, Marie Kayser-Potts and Dr. Michael Sennett for M_w and Raman measurements, Professor William Orme-Johnson and co-workers for help with ESR measurements, Digital Equipment Corp. for donation of the PRO-350 computer and peripherals, and Dr. Mark Schure for system programming. Finally, M.A.E.-S. thanks Alexandria University for study leave.

Registry No. D, 97731-71-0; 2,6-dimethylphenol, 576-26-1.

Supplementary Material Available: Plot of 10^3DIFF (kcal deg^{-1} mol^{-1}) vs. $\Delta H_{11}^{\bullet}$ (kcal mol^{-1}) (1 page). Ordering information is given on any current masthead page.

Contribution from the University Chemical Laboratory, Cambridge CB2 1EW, U.K.

Ligand Fields from Misdirected Valency. 4. Magnetic Susceptibilities and Electron Spin Resonance and Optical Spectra of Tetrakis(diphenylmethylarsine oxide)(nitrato)cobalt(II) and -nickel(II) Nitrates

Neil D. Fenton and Malcolm Gerloch*

Received March 5, 1987

Ligand-field analyses of $[M(OAsPh_2Me)_4NO_3]^+NO_3^-$ (M = Co(II), Ni(II)) have accurately and simultaneously reproduced the principal crystal susceptibilities and their temperature variations in the range 80–300 K, the d–d optical transition energies, and, for the cobalt complex, the principal molecular g values and their orientations. A cellular ligand-field approach has been based upon a recent crystallographic reanalysis. Substantial values for local $e_{\pi\sigma}$ parameters for both ligand types evidence the misdirected nature of the local metal–oxygen interactions arising from bent bonding and/or contributions from oxygen nonbonding lone pairs. Detailed differences between values of $e_{\pi\parallel}$ (referring to the misdirected valence) are argued to reflect slightly more polarization of the metal–oxygen bonds toward the nickel atom than toward the cobalt. The same greater effective nuclear charge in the d^8 complex is accompanied by a relative increase in the axial metal–oxygen bonding and ligand field in that complex.

Introduction

In 1965 the preparation of the complexes $M(Ph_2MeAsO)_4X_2$ (M = Co(II), Ni(II); X = NO_3^-, ClO_4^-) was reported,[1] together with a preliminary X-ray structural analysis[2] that characterized their pentacoordination geometry as being of the square-based pyramidal type. One nitrate or perchlorate group bonds to the metal atom in the apical site while the other forms an anion of crystallization. Since then extensive studies of all important ligand-field properties of these molecules have been investigated. The paramagnetic susceptibilities and anisotropies of the tetragonal crystals have been measured[3,4] in the temperature range 300–80 K for the nitrate complexes of both metals together with single-crystal, polarized optical spectra[3,4] at 20, 80, and 300 K. More recently, Bencini et al.[5] have presented a careful study of the single-crystal ESR **g** tensors of $[Co(Ph_2MeAsO)_4NO_3]^+NO_3^-$. The early X-ray study placed the metal atoms in these complexes on crystal tetrads, so requiring disorder of the apical perchlorate or nitrate donors. The ESR study monitored the ensuing lower molecular symmetry uniquely within the ligand-field measurements, revealing a very large in-plane anisotropy for the **g** tensor.

Hitherto, two ligand-field analyses have been published. The earlier one[3,4] reproduced the principal crystal susceptibilities and d–d transitions in the optical spectra within the global and approximate parameterization scheme in fourfold symmetry in terms of variables such as *Dq*, *Ds*, and *Dt*. The potentially much more revealing parameterization of the Angular Overlap Model (AOM) was employed by Bencini et al.[5] in the more recent study. A good account of the principal g values and their orientations was provided for the cobalt system, but only fair reproduction of the optical spectrum was achieved. The correct sign of the crystal paramagnetic anisotropy was predicted, but quantitative agreement with experiment was lacking. The "best-fit" AOM parameter set was reported[5] as follows: $e_\sigma(NO_3)$ = 6015 cm^{-1}, $e_{\pi\perp}(NO_3)$ = 1580 cm^{-1}, $e_{\pi\parallel}(NO_3)$ = 3950 cm^{-1}, e_σ(AsO) = 6685 cm^{-1}, e_π(AsO) = 2765 cm^{-1}, B = 760 cm^{-1}, k = 0.9, ζ = 533 cm^{-1}. Shortcomings of this analysis are apparent in the use of an isotropic treatment for e_π(AsO); the very large value of the ligand-field trace Σ (defined[6,7] as the sum of all diagonal e values in a given complex) of 60 405 cm^{-1} as compared with values around 22 000 cm^{-1} for many other cobalt(II), nickel(II), and copper(II) systems;[8] and the neglect of the misdirected nature of all the metal–oxygen interactions in these species. Earlier papers[9-11] in this series have established the need to recognize both bent bonding and the role of nonbonding donor-atom long pairs in ligand-field studies. Their neglect can affect both the efficacy and significance of such analyses markedly.

The present analysis seeks to provide good agreement with all experimental ligand-field properties and achieves this in a manner that is consistent with a wide and growing body of similar ligand-field analyses within what we now call the Cellular Ligand-Field (CLF) model.

(1) Lewis, J.; Nyholm, R. S.; Rodley, G. A. *Nature (London)* **1965**, *207*, 72.
(2) Pauling, P.; Robertson, G. B.; Rodley, G. A. *Nature (London)* **1965**, *207*, 73.
(3) Gerloch, M.; Kohl, J.; Lewis, J.; Urland, W. *J. Chem. Soc. A* **1970**, 3269.
(4) Gerloch, M.; Kohl, J.; Lewis, J.; Urland, W. *J. Chem. Soc. A* **1970**, 3283.
(5) Bencini, A.; Benelli, C.; Gatteschi, D.; Zanchini, C. *Inorg. Chem.* **1979**, *18*, 2526.
(6) Deeth, R. J.; Gerloch, M. *Inorg. Chem.* **1985**, *24*, 1754.
(7) Woolley, R. G. *Chem. Phys. Lett.* **1985**, *118*, 207.
(8) Deeth, R. J.; Gerloch, M. *J. Chem. Soc., Dalton Trans.* **1986**, 1531.
(9) Deeth, R. J.; Duer, M. J.; Gerloch, M. *Inorg. Chem.* **1987**, *26*, 2573.
(10) Deeth, R. J.; Duer, M. J.; Gerloch, M. *Inorg. Chem.* **1987**, *26*, 2578.
(11) Deeth, R. J.; Gerloch, M. *Inorg. Chem.* **1987**, *26*, 2582.

0020-1669/87/1326-3273$01.50/0

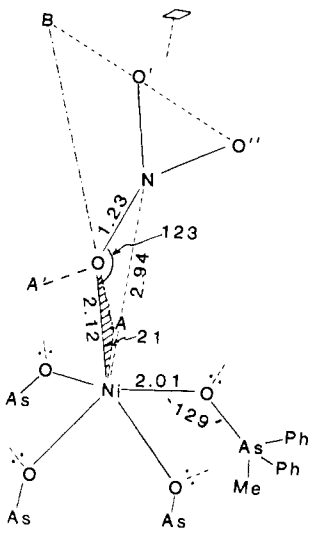

Figure 1. Coordination in $[Ni(OAsPh_2Me)_4NO_3]^+NO_3^-$. The four arsine oxide ligands are related by a crystallographic tetrad upon which also lies the nickel and nitrogen atoms. The nitrate ligands (refined[13] as rigid bodies) are disordered between four rotationally related sites. OA and OA′ represent the directions of oxygen sp^2 lone pairs in the plane of the nitrate group. AO produced meets O″O′ produced at B in the same plane. AB is the line of intersection of planes NiAO and the nitrate ligand. O′O″ and O′B are of equal length.

Bases, Geometry and Parameters

All calculations have been performed within the CAMMAG2 system,[12] employing the CLF model, within bases spanning $^4F + {}^4P$ for the cobalt nitrate system or $^3F + {}^3P$ for the nickel nitrate complex. Later refinements were performed within the full d^7 or d^8 configuration bases, as appropriate and noted in the text below.

CLF (and AOM) analyses parameterize ligands in their actual coordination sites and orientations. Bencini et al.[5] were obliged to make informed guesses of the detailed coordination geometry, for the original preliminary X-ray analysis[2] did not provide it and had not been followed with a full report. In particular, the coordination of the apical nitrate group was itself parameterized in terms of two polar angles, although the origins of that frame within the actual crystal were not clearly explained. Altogether, it was clear at the outset that no reliable ligand-field analysis would be possible without a detailed structural analysis: this is, of course, the usual prerequisite in this sort of study. Accordingly, we rely here on the isomorphism[2] between $[M(Ph_2MeAsO)_4NO_3]^+NO_3^-$ (M = Co(II), Ni(II)) together with a recent reanalysis[13] of the X-ray diffraction of the nickel nitrate system. Some relevant features of that analysis are shown schematically in Figure 1.

The metal atom lies on a crystallographic tetrad some 0.4 Å above the square plane defined by the oxygen donors of the substituted arsine oxides. The nitrates are required to be disordered equally between four rotationally related sites, and the central nitrogen atom lies on the fourfold axis. The nitrate groups were refined in the X-ray analysis[13] as rigid bodies with exact local threefold planar symmetry. The metal atom lies close (0.38 Å) to, but not exactly in, the plane of the nitrate ligand so that misdirected valence between the metal and the donor oxygen is likely for this reason alone. Further bent bonding might also derive from the angle ∠NiON not being 120°, though it is close. Since the enormous anisotropy observed in the molecular **g** tensor normal to the tetrad (Table II) must arise from the nonaxial nature of the Ni–ONO_2 bonding, it is important to construct a local M–NO_3 coordinate frame, with respect to which CLF *e* parameters are defined, that best reflects the likely local bonding. As usual, the local *z* axis is taken along the O–Ni vector and we have defined

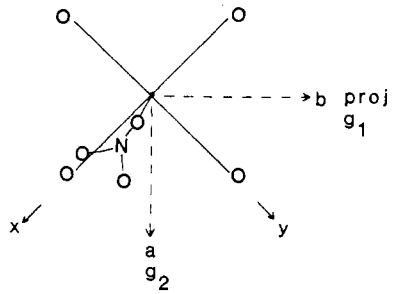

Figure 2. Orientations of the crystal *a*, *b*, *c* axes, the molecular *x*, *y*, *z* axes, and the observed **g** tensor in $[Co(OAsPh_2Me)_4NO_3]^+NO_3^-$. The crystallographic *c* and coincident molecular *z* axes lie normal to the page toward the viewer. The principal g_2 value lies parallel to *a*. The projection of g_1 onto the *ab* plane lies parallel to *b*: g_3 is directed into the page at 11.5° to the normal and in the *bc* plane (see Table II).

y as perpendicular to the NiOA plane so that the local ligand field is parameterized by e_σ and $e_{\pi\perp}$ ($\equiv e_{\pi y}$) to represent σ and π interactions, together with $e_{\pi\sigma}$ and $e_{\pi\parallel}$ to reflect the misdirected valence, as in part 1[9] of this series. Thus $e_{\pi\sigma} = \langle d_{xz}|V_{LF}|d_{z^2}\rangle$ and $e_{\pi\parallel} = \langle d_{xz}|V_{LF}|d_{xz}\rangle$.

These axis orientations were communicated to the computer program—CAMMAG2—by a standard convention[14] in which the local *z* axis lies parallel to the first two named atoms in a triad and *y* is perpendicular to the plane defined by the triad. From the construction shown in Figure 1, the triad NiOB effects the desired definitions. The length of OA is not required. This construction is founded upon the assumed value of 120° for ∠AON and sp^2 hybridization at the donor oxygen atom. Any inadequacy in that assumption will carry over to the choice of point B in the defining triad and ultimately in some, clearly small, rotation of the local ligand frame about the Ni–O vector. This issue is addressed later.

The local ligand frames for the arsine oxide ligands are defined by the triads NiOAs so that $e_{\pi\sigma}$(OAs) is expected to account for the ligand-field effects of the nonbonding lone pair on the donor oxygen atom, as in part 1[9] of this series.

The complete list of CLF parameters throughout these analyses is therefore as follows: $e_\sigma(NO_3)$, $e_{\pi\perp}(NO_3)$, $e_{\pi\parallel}(NO_3)$, $e_{\pi\sigma}(NO_3)$, e_σ(AsO), $e_{\pi\perp}$(AsO), $e_{\pi\parallel}$(AsO), $e_{\pi\sigma}$(AsO). In addition, we parameterize interelectron repulsions with *B* and *C* (F_2 and F_4), spin–orbit coupling with the one-electron coefficient ζ, and the magnetic moment operator with Stevens' orbital reduction factor *k*, as usual.

CLF Analyses

Preliminary calculations quickly showed that approximately satisfactory reproduction of the optical spectra of both nickel and cobalt complexes can be obtained within fairly wide variations of the parameter set. In view of the high degree of parameterization this is not surprising. It was equally clear, however, that reproduction of the observed[5] **g** tensor for the cobalt complex was far more exacting, and so the detailed analysis begins with that property.

Initially calculations were performed within the restricted maximum spin-degeneracy basis $^4F + {}^4P$, for reasons of economy. Wide variations of all parameters showed that reproduction of both principal *g* values and their orientations (Figure 2) was very difficult to achieve. This was, of course, fortunate, for it offered the possibility of a unique "fit". It was immediately clear that even approximately good fits to the **g** tensor require substantial values for the $e_{\pi\sigma}$ parameters of both ligand types: similar conclusions emerged in the earlier studies in this series.[9-11] Accurate reproduction required variation of all parameters. The large in-plane *g* anisotropy is therefore a result of the nonaxial nature of the Co–nitrate coordination compounded with the details of the ligand fields of the basal ligands: this was not unexpected. The calculated **g** tensor is sensitive to all parameter

(12) "CAMMAG2", a FORTRAN program by A. R. Dale, M. Gerloch, and R. F. McMeeking.
(13) Falvello, L. R.; Gerloch, M.; Raithby, P. R. *Acta Crystallogr.*, in press.
(14) Gerloch, M. *Magnetism and Ligand-Field Analysis*; Cambridge University Press: Cambridge, England, 1983; Chapter 9.

Table I. Parameter Values Affording Optimal Reproduction of Crystal Susceptibilities, Molecular **g** Tensors (for the Cobalt Complex), and d–d Transition Energies in $[M(OAsPh_2Me)_4NO_3]^+NO_3^-$ (M = Co(II), Ni(II); Estimated Errors in Parentheses)

parameter	Co complex	Ni complex
$e_\sigma(AsO)/cm^{-1}$	3500 (200)	3550 (50)
$e_{\pi\perp}(AsO)/cm^{-1}$	980 (100)[c]	950 (100)
$e_{\pi\parallel}(AsO)/cm^{-1}$	875 (30)	675 (100)
$e_{\pi\sigma}(AsO)/cm^{-1}$	945 (100)[d]	880 (50)
$e_\sigma(NO_3)/cm^{-1}$	100 (200)	1700 (250)
$e_{\pi\perp}(NO_3)/cm^{-1}$	−200 (100)	100 (100)[e]
$e_{\pi\parallel}(NO_3)/cm^{-1}$	650 (200)	350 (150)[f]
$e_{\pi\sigma}(NO_3)/cm^{-1}$	950 (200)	1650 (200)[g]
Σ/cm^{-1}	21970 (1200)	22850 (1200)
B/cm^{-1}	850 (30)	940 (20)
C/cm^{-1}	3600 (100)	3450 (100)
$F_2{}^a/cm^{-1}$	1364 (35)	1433 (35)
$F_4{}^a/cm^{-1}$	103 (3)	99 (3)
ζ/cm^{-1}	513 (20)	533 (30)
k	0.9 (0.05)	0.8 (0.05)
α^b/cm^{-1}	50	50

[a] Slater–Condon–Shortley Parameters are related to the Racah parameters by $B = F_2 - 5F_4$ and $C = 35F_4$. [b] The Trees correction was held fixed at 50 cm^{-1} and not refined or determined by these analyses. [c] Optimal parameters are correlated by $e_{\pi\perp}(AsO) = 0.5e_\sigma(AsO) - 770$ cm^{-1}. [d] Optimal parameters are correlated by $e_{\pi\sigma}(AsO) = -0.33e_\sigma(AsO) + 2100$ cm^{-1}. [e] Optimal parameters are correlated by $e_{\pi\perp}(NO_3) = -0.5e_\sigma(NO_3) + 3715$ cm^{-1}. [f] Optimal parameters are correlated by $e_{\pi\parallel}(NO_3) = -e_\sigma(NO_3) + 2000$ cm^{-1}. [g] Optimal parameters are correlated by $e_{\pi\sigma}(NO_3) = -1.25\ e_\sigma(NO_3) + 3715$ cm^{-1}.

Table II. Comparison between the Observed[5] **g** Tensor in the Cobalt Complex and That Calculated with the Optimal Parameter Set in Table I

obsd[a]				calcd			
	angle, deg, subtended with axes				angle, deg, subtended with axes		
	a	*b*	*c*		*a*	*b*	*c*
$g_1 = 8.6$	90	11.5	77.5	$g_1 = 8.59$	90	11	79
$g_2 = 1.3$	0	90	90	$g_2 = 1.29$	1	90	89
$g_3 = 0.91$	90	77.5	168.5	$g_3 = 0.93$	89	79	169

[a] The quoted orientation refers to a crystallographically equivalent but magnetically different site from that given in Table I of ref 5.

combinations—so engendering lengthy analysis—but especially to the combination of $e_\sigma(AsO)$ with $e_{\pi\perp}(AsO)$. Accordingly, these last two parameters are the ones more accurately determined by the ESR experiment.

However, within the ranges of correlated parameters that yield acceptable reproduction of the **g** tensor, most combinations fail utterly to account for the paramagnetic susceptibilities.[4] The electronic spectrum[4] provided a less exacting task except in the later stages of the analysis when more precise reproduction of experiment was sought. Satisfactory accounts of the three sets of experimental data—susceptibilities, **g** tensor, and absorption spectrum—were obtained with different combinations of parameters, and refinement began by searching for a region of parameter space that reproduced all properties simultaneously. It is desirable to encounter circumstances in which a larger data base focuses an analysis in this way, especially in view of the larger number of parameters employed, but it is sad to note their rarity. A common region of parameter space was located eventually, at which stage in the analysis the computational basis was enlarged to the full set of 120 states spanned by the d^7 configuration. The effects of the spin doublets upon calculated susceptibilities in the fitting region were quite significant, a circumstance also found for other systems.[15] Changes in computed *g* values were less marked but were nevertheless important. All calculations from this stage included the doublets. Parameter values that best fit the principal crystal susceptibilities and their temperature dependence, the principal molecular ESR *g* values and their orientations, and the d–d transition energies are listed in Table I. Comparisons between the observed properties and those calculated with these "best-fit" parameter values are presented in Tables II–IV.

Included in Table I is a value of $\alpha = 50$ cm^{-1} for the Trees correction[16] for electron correlation effects in our account of the Coulomb interactions. The importance of this correction has been demonstrated elsewhere[17] for some manganese(II) complexes. Even though the present analyses cannot support any refinement of the Trees parameter, an estimate of 50 cm^{-1}, as compared with free-ion values[18] of around 70 cm^{-1}, seems more defensible than its total neglect. Inclusion of the fixed Trees correction merely affects the Racah parameters that otherwise emerge from these analyses. The value of Racah's *C* parameter was determined in the present analysis simply by its optimization to reproduce the spin-forbidden band at 18 700 cm^{-1} after all other parameters were held fixed at their previously determined values.

For the nickel(II) analogue, reproduction of the principal crystal susceptibilities and their temperature variations[3] and of the d–d spectrum[3] was undertaken as a completely separate exercise. While, in the cobalt analysis, fitting the **g** and susceptibility tensors

Table III. Comparison between Observed[3,4] d–d Transition Energies (cm^{-1}) and Those Calculated with the Optimal Parameter Sets in Table I[a]

spin mult	energy calcd	energy obsd	spin mult	energy calcd	energy obsd
		Cobalt Complex			
2	23 853		4	16 560	16 600
2	23 522		2	16 332	
2	22 973		2	16 017	
2	22 559		2	13 330	
4	20 650	20 500	2	12 142	
2	20 212		4	10 425	11 300
2	19 626		2	10 257	
2	18 669	18 700	4	7342	6900
2	18 333		4	6426	
2	17 689		4	2524	
2	17 345		4	1897	
4	16 900	17 000	4	837	
2	16 698		4	0	
		Nickel Complex			
3	23 229	22 900	3	12 188	11 900
3	22 531		3	11 462	
1	22 130		1	10 864	
1	20 933		3	9362	9300
3	19 150	19 000	3	7846	8200
1	17 024	17 000	3	4463	
1	15 830		3	2682	
1	13 705	13 690	3	0	

[a] Calculated transitions are averaged over spin multiplets and listed up to 24 000 cm^{-1}. Zero-field splittings are calculated for the cobalt ground quartet at 146.77 cm^{-1} and for the nickel ground triplet at 19.05 and 54.28 cm^{-1}.

Table IV. Comparison between Observed[3,4] Crystal Susceptibilities (χ/cgsu × 10^{-4}) and Those Calculated with the Optimal Parameter Sets in Table I

temp/K	Co complex $\chi_\parallel$ obsd	Co complex $\chi_\parallel$ calcd	Co complex $\chi_\perp$ obsd	Co complex $\chi_\perp$ calcd	Ni complex $\chi_\parallel$ obsd	Ni complex $\chi_\parallel$ calcd	Ni complex $\chi_\perp$ obsd	Ni complex $\chi_\perp$ calcd
300	65	62	128	135	40	40	52	52
200	86	81	194	204	59	58	77	78
140	96	98	283	295	80	80	111	110
100	108	113	395	413	105	106	156	155

(15) Mackey, D. J.; Evans, S. V.; McMeeking, R. F. *J. Chem. Soc., Dalton Trans.* **1978**, 160.

(16) Trees, R. E. *Phys. Rev.* **1951**, *83*, 756.

(17) Dale, A. R.; Gerloch, M., manuscript in preparation.

(18) Shadini, Y.; Caspi, E.; Oreg., J. *J. Res. Natl. Bur. Stand., Sect. A* **1969**, *73A*, 103.

proved to be more exacting than fitting the optical spectrum, reproduction of the d–d transition energies in the nickel system emerged as the harder task. In due course, a common region of parameter space providing a good account of all experimental data was identified. As for the cobalt analysis, refinement was completed within the full configurational basis. Inclusion of the spin singlets of d^8 generally had a less marked effect upon the "best-fit" parameter set than did inclusion of the doublets in the cobalt system. The optimal parameter set is included in Table I, and comparisons between observed and calculated electronic properties are made in Tables II–IV.

The estimated errors quoted for the parameter values in Table I represent tolerances outside of which some or all of the calculated properties lie unacceptably far from those determined by experiment, as judged subjectively by comparison with the wide range of ligand-field analysis now available. In some cases, however, optimal parameter values are correlated as noted in the footnotes of Table I. That so many parameters have been reasonably well determined by these analyses is fortunate and undoubtedly arises from the large data base afforded by the wide range of electronic properties studied.

Finally, in the previous section was raised the issue of the choice of local y axis for the nitrate group in case the oxygen donor lone pair is not directed exactly along OA of Figure 1. In those circumstances the plane NiOA and chosen y axis will be rotated slightly about the Ni–O vector. In the program package[12] CAMMAG2, this can be effected directly by rotation of the local ligand-field potential (expressed as a superposition of spherical tensors in the usual way) about the metal–oxygen vector. In the present analyses, such rotations by up to 2° for the cobalt system have little effect but are disadvantageous outside those limits; in the nickel system, rotations by 5° can be tolerated before fits deteriorate significantly. We conclude that our chosen local axis frame has been well chosen and that the local oxygen donor lone pair does not lie far from the "ideal" sp^2 orientation.

Discussion

Elsewhere,[6,8] we have demonstrated empirically that values for the ligand-field trace Σ ($\equiv \Sigma^{\text{ligands}} \Sigma_{\lambda=\sigma,\pi_x,\pi_y}{}^{\text{modes}} e_\lambda$) are remarkably independent of coordination number or even, for the latter half of the first transition-metal series in oxidation state II at least, of the cental metal atom. This sum rule, which has received theoretical attention[7] also, is founded upon complexes with ligands of the amine, chloro, and oxo types: recent unpublished work by our group suggests that some systematic variations in Σ values might accompany changes to significantly different ligand groups. Meanwhile, the typical value $\Sigma \approx 22\,000$ cm^{-1} established thus far is confirmed by the present studies in analyses that were completed independently of each other or of any other. We believe increasingly that this result confers, of itself, confidence in the remaining optimal parameter values.

The ligand fields of both ligand types in both complexes are characterized by substantial values for $e_{\pi\sigma}$. These analyses thus confirm the roles of bent bonding and of nonbonding donor-atom lone pairs that were established by the earlier papers[9-11] of this series. The positive sign for $e_{\pi\sigma}$(AsO) correlates, via the definitions in part 1,[9] with the origin of the misdirected valence lying in the oxygen nonbonding lone pair (i.e. sited along the negative sense of the local x axis) and/or in any bent bonding on the same side of the metal–oxygen vector. As ∠MOR angles commonly exceed 120° and relatively unhindered, if small, rotations of the nonchelating arsine oxide ligand about the metal–oxygen vector appear possible, we suppose that M–O bonding overlap has been maximized and that any bent bonding is minimal. Bent bonding seems likely, however, in the M–O interaction with the nitrate ligand because the metal atom does not lie in the ligand plane. The frame-defining choice of the triad NiOB, discussed above, orients the local x axis on the opposite side of the M–O vector to the donor, lone-pair direction OA so that the resulting bent bonding should define a positive value for $e_{\pi\sigma}(NO_3)$; this also emerges in the analysis. Any contribution to that parameter from the nonbonding oxygen lone pair would be negative in this frame, so we conclude that the misdirected-valence effects are dominated by the bent bonding here.

The $e_{\pi\perp}$ values in Table I illustrate how, again for both cobalt and nickel species, the arsine oxide ligands function as π donors while little if any π functionality is evident for the nitrate groups. The large values for $e_{\pi\parallel}(NO_3)$ do not gainsay this, of course, for they must be presumed to arise as a consequence of the misdirected valency: we discuss this further below.

The most obvious difference between the optimal parameter sets of the cobalt and nickel systems concerns the values of $e_\sigma(NO_3)$—100 and 1700 cm^{-1}, respectively. First we note that these numbers represent the sum of e_σ values for nitrate and the coordination void sited diametrically opposite. The ligand-field contributions from coordination voids has been addressed[19] in detail recently. In planar metal(II) systems, the d–s interaction appears to be characterized with e_σ(void) around −3000 to −3500 cm^{-1}. In the square-based pyramidal $[Cu(NH_3)_5]^{2+}$ ion, $e_\sigma(NH_3) + e_\sigma$(void), corresponding to the $e_\sigma(NO_3)$ parameter here, was found[19] as −750 cm^{-1}, although the Cu–N bond in the axial site of that molecule is markedly longer than in the equatorial one. Overall, therefore, the $e_\sigma(NO_3)$ values given in Table I do not indicate small or negligible M–O interactions, for, after a notional "correction" for the void, these values might well be in the region 3500 and 5200 cm^{-1}, respectively. We therefore address the difference between these values rather than their absolute magnitudes. At the same time we consider the simultaneous decrease in $e_{\pi\parallel}$ values on replacing cobalt by nickel.

We expect that the major consequences of traversing the transition series from left to right are the increasing effective nuclear charge and decreasing covalent radius due to both poor d-shell self-shielding and increasing penetration effects for the valence s(p) functions. Current understanding[14] of the origin of ligand fields identifies the major contribution to any CLF (or other ligand-field model) parameter as arising from that region of space most shared by the bond orbital and relevant d orbital. The bond orbital, essentially describing the interaction of the metal s (and p) function with appropriate (σ, π, ...) ligand functions, will grow a little more metallike with increasing effective nuclear charge. At the same time the local d orbital will be contracted somewhat. We might therefore expect that any misdirected valency, as illustrated in Figure 1 of part 1[9] of this series, would appear less off-axis. Recalling that $e_{\pi\parallel} \approx |\langle d_{xz}|V|\chi\rangle|^2/(\epsilon_d - \bar{\epsilon}_\chi)$ and $e_{\pi\sigma} \approx \langle d_{xz}|V|\chi\rangle\langle\chi|V|d_{z^2}\rangle/(\epsilon_d - \bar{\epsilon}_\chi)$, the expected decrease in $\langle d_{xz}|V|\chi\rangle$ will be offset to some extent by a simultaneous increase in $\langle d_{z^2}|V|\chi\rangle$ with general orbital contraction. The decrease by 200 cm^{-1} of $e_{\pi\parallel}$(AsO) but by only 65 cm^{-1} in $e_{\pi\sigma}$(AsO) on replacement of cobalt by nickel might thus be an indicator of increased effective nuclear charge and polarization of the bond more toward the metal, as would be the decrease by 300 cm^{-1} in $e_{\pi\parallel}(NO_3)$ that accompanies the large increase in $e_{\pi\sigma}(NO_3)$. The large value of $e_{\pi\sigma}$ here is undoubtedly associated with the large increase in $e_\sigma(NO_3)$ that we emphasized above and to which we now return.

The same increased effective nuclear charge of nickel(II) compared with that of cobalt(II) is expected to be accompanied by some bond shortening and increased ligand-field strength. Whether such changes take place isotropically or not depends on many factors, including the basic change of asymmetry in the repulsive role of the partly filled d shell. The response of geometry and ligand fields to the changing occupancy of the d shell in complexes has been demonstrated and reviewed recently.[20,22] The ordering of the d orbitals in the present square pyramidal complexes is expected to be $E(d_{x^2-y^2}) > E(d_{z^2})$ and $E(d_{xy}) > E(d_{xz,yz})$, the former inequality arising from the weak *net* axial field offered by only one ligand plus the negative void effect and the latter occurring if, as here, the ligands offer donation perpendicular to the M–O–As planes, which are themselves approximately normal

(19) Deeth, R. J.; Gerloch, M. *Inorg. Chem.* **1984**, *23*, 3846.
(20) Deeth, R. J.; Gerloch, M. *Inorg. Chem.* **1984**, *23*, 3853.
(21) Deeth, R. J.; Gerloch, M. *Inorg. Chem.* **1986**, *24*, 4490.
(22) Gerloch, M. In *Understanding Molecular Properties*; Avery, J. S., Hansen, A., Dahl, J. P., Eds.; Riedel: Dordrecht, The Netherlands, 1987; p 111.

Table V. Calculated Spin-Quartet Transition Energies (cm^{-1})

set A: 0, 820, 1844, 3449, 6637, 7476, 10778, 16097, 16682, 22215
set B: 0, 865, 2262, 3935, 6583, 7926, 12135, 15260, 17919, 22242

to the global basal coordination plane. In the strong-field limit, the change cobalt → nickel is accompanied by the configurational change $(d_{xz,yz})^4(d_{xy})^1(d_{z^2})^1(d_{x^2-y^2})^1 \rightarrow (d_{xz,yz})^4(d_{xy})^2(d_{z^2})^1(d_{x^2-y^2})^1$ and hence by increased d-shell repulsion in the basal plane. The greater Lewis acidity would then be expected to be satisfied more easily by shortening of the axial ligation and accompanied by an increased e_σ(axial) value, as observed. It is the case, however, that the characters of the lowest three orbitals, which do indeed correspond predominantly to $t_{2g}(O_h)$ parentage, are considerably intermixed, partly as a result of the metal not lying in the basal plane defined by the arsine oxide oxygen atoms and partly because of the complex orbital interactions that accompany the local, misdirected valency. We must be content, therefore, merely to observe the increased axial ligand field in the nickel complex; we expect a determination of the structure of the cobalt molecule by X-ray methods to reveal a Co–ONO_2 bond length longer than the Ni–ONO_2 one of 2.09 Å.

These ideas are lent support by the facts and discussion of earlier analyses[23] of the spectra and paramagnetism of $M(L_N^+)X_3$ species (M = Co(II), Ni(II); X = Cl, Br; L_N^+ = the tertiary bicyclic amine dabconium). Those complexes possess trigonally distorted tetrahedral coordination. As one passes from the cobalt to the nickel system, the e_σ(axial) value increases markedly (by ca. 1900 cm^{-1}) as the M–L_N^+ bond shortens, while little change in either bond length or ligand-field strength occurs for the basal ligands. The parallel with the present systems is close.

In summary, the present ligand-field analyses, though highly parameterized, yield essentially unique optimal parameter values while rationalizing a great deal of independent experimental data. The analyses were performed independently, and their conclusions appear to fit well with general perceptions of transition-metal bonding. The broad agreement between the parameter sets for the cobalt and nickel analogues confirms the similar nature of the complexes, and the numerical values are unexceptional when compared widely throughout the transition-metal series. The detailed differences between the two parameter sets do not seem merely to reflect analytical inadequacy but rather correlate well with other systems and with centrally important electronic differences between d^7 and d^8 species.

The degree of parameterization in these analyses may, at first sight, cause concern on two counts: first, by virtue of the large number (12) of ligand-field variables employed, and second, in view of the earlier AOM analysis[5] of Bencini et al. having reproduced the observed **g** tensor rather well. Bencini et al. were obliged to guess some details of the molecular geometry and to parameterize others. Tables V–VII list ligand-field properties calculated with Bencini et al.'s AOM parameter values together with the actual coordination geometry that has recently become available.[13] The **g** tensor is not well reproduced, susceptibilities are better accounted for than suggested in ref 5, and agreement between observed and calculated d–d transition energies is poor. By contemporary standards these fits are not acceptable. However, the close reproduction of all data shown in Tables II–IV apparently arises from a much more highly parameterized model. Whether the number of parameters employed really *is* greater depends upon whether or not one accepts that assumptions define parameters in themselves. Thus, the use of an isotropic e_π parameter for the arsine oxide ligations is not so much of a simplifying assumption as a restriction denying the likely (though small as it turns out) asymmetry of these interactions. Similarly, the omission of all reference to the $e_{\pi\sigma}$ parameters corresponds analytically to the assumption that all $e_{\pi\sigma} = 0$. If such was acceptable in 1979, it surely cannot be today when the ligand-field consequences of misdirected valency and of nonbonding lone pairs on donor atoms have been demonstrated unequivocally in other systems.[9-11] The present analyses have defined values for the $e_{\pi\sigma}$ parameters that accord well with the placing of lone pairs on the one hand or with the misdirected nitrate ligation on the other.

(23) Gerloch, M.; Manning, M. R. *Inorg. Chem.* **1981**, *20*, 1051.

Table VI. Calculated **g** Tensor

	orientation, deg, with respect to axes					
	calcd			best exptl[a]		
g	*a*	*b*	*c*	*a*	*b*	*c*
			Set A			
8.78	27.4	63.1	95.0	11	90	77
0.53	117.0	27.0	90.3	90	0	90
0.43	85.7	87.5	5.0	77	90	168
			Set B			
8.59	68.2	156.6	98.2	90	168	102
0.86	22.2	69.3	82.4	0	90	90
0.67	86.0	79.6	168.8	90	70	168

[a] Chosen from magnetically equivalent sites without heed to handedness.

Table VII. Calculated Crystal Susceptibilities (χ/cgsu × 10^{-4})

	set A		set B	
temp/K	$\chi_\parallel$	$\chi_\perp$	$\chi_\parallel$	$\chi_\perp$
300	55	130	55	128
200	69	199	70	195
140	80	287	82	281
100	87	402	92	393

This series has addressed the ligand-field manifestations of misdirected valency. Independent analyses of 10 different molecules with varying coordination number, geometry, and metal have each demonstrated the sensitivity of ligand-field properties to bonding details previously considered too subtle to be observed in this way. We have discussed the nontransferability of ligand-field parameters many times.[8-11,14,19-22] The present analyses demonstrate again that it is the bonding principles that underlie our interpretation of the parameters that are transferable rather than the parameter values themselves. Nevertheless, we do not expect large differences between broadly similar systems. In this respect, the large values for e_π(Co–NO_3) proposed by Bencini et al.[5] are immediately disquieting. So too, in the light of more recent work on the ligand-field contributions of coordination voids,[19] is the large value proposed[5] for the axial e_σ(Co–NO_3) parameter. The one ligand-field quantity that does seem to be transferable between systems (though this is still under active investigation) is the trace Σ. Values here of ca. 22000 cm^{-1} accord well with a score or more of similar values determined for other cobalt(II), nickel(II), and copper(II) complexes,[8,11] a result offering further support for the consistency of the present approach[22] with ligand-field theory and bonding. The contrast with the trace Σ = 60405 cm^{-1}, characterizing the earlier analysis,[5] is stark.

Acknowledgment. N.D.F. thanks the SERC for a Research Studentship.

Appendix

Tables V–VII list ligand-field properties for $[Co(Ph_2MeAsO)_4NO_3]^+NO_3^-$ calculated by using atomic coordinates from a recent determination[13] of the X-ray crystal structure of the nickel(II) analogue, together with the ligand-field parameters of Bencini et al.[5] Results are tabulated for two sets of parameter values, reflecting uncertainty in the association of $e_{\pi c}$ and $e_{\pi s}$ with the directions chosen by us for $e_{\pi\parallel}$ and $e_{\pi\perp}$. The parameter lists are as follows.

Set A: e_σ(AsO) = 6685 cm^{-1}, e_π(AsO) = 2765 cm^{-1}, $e_\sigma(NO_3)$ = 6015 cm^{-1}, $e_{\pi\parallel}(NO_3)$ = 3950 cm^{-1}, $e_{\pi\perp}(NO_3)$ = 1580 cm^{-1}, B = 760 cm^{-1}, ζ = 533 cm^{-1}, k = 0.85.

Set B: the same as set A, except that $e_{\pi\parallel}(NO_3)$ = 1580 cm^{-1} and $e_{\pi\perp}(NO_3)$ = 3950 cm^{-1}.

Registry No. $[Co(OAsPh_2Me)_4NO_3]^+NO_3^-$, 18712-88-4; $[Ni(OAsPh_2Me)_4NO_3]^+NO_3^-$, 109583-99-5.